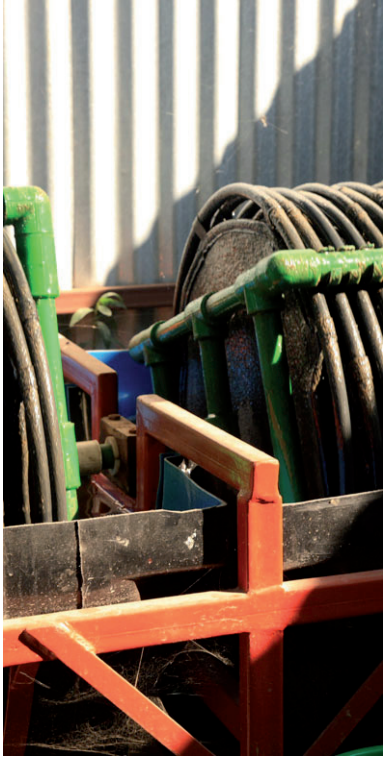

Low-cost Rotating Biological Contactor

Construction Manual

eawag aquatic research

Eawag – Swiss Federal Institute of Aquatic Science and Technology

UN-HABITAT FOR A BETTER URBAN FUTURE

UN-HABITAT – United Nations Human Settlement Programme

Low-cost Rotating Biological Contactor – Construction Manual

Contributing Authors: Marijn Zandee, Bastian Etter, Kai Udert

This report documents the design, building and testing process of a pilot RBC reactor constructed with locally available materials in Nepal. The intention is that it can serve as a manual to construct similar wastewater treatment units in Nepal and other parts of the world.

STUN is a collaboration of:
Eawag – Swiss Federal Institute of Aquatic Science and Technology
Überlandstrasse 133
8600 Dübendorf
Switzerland
Tel: +41 44 823 50 48 Fax: +41 44 823 50 28

UN-Habitat – The United Nations Human Settlement Programme
PO Box 107
Kathmandu
Nepal
Tel: +977 1 55 42 816 Fax: +977 1 55 39 877

For further information visit: *www.eawag.ch/stun*

January 2011 – Māgh 2067

1 Index

Acronyms

Anammox	Anaerobic ammonium oxidation
EcoSan	Ecological sanitation
Eawag	Swiss Federal Institute of Aquatic Science and Technology, Dübendorf, Switzerland
HDPE	High density polyethylene (plastic pipe material)
N	Nitrogen
NRs	Nepalese Rupee (approx 96 NRs to one Euro at time of writing)
P	Phosphorus
PE	Polyethylene (plastic material)
PP-R	Polypropylene random copolymer (plastic piping material)
PU	Polyurethane (plastic foam)
PVC	Polyvinyl chloride (plastic piping material)
RBC	Rotating biological contactor
RPM	Revolutions per minute
STUN	Struvite recovery from urine in Nepal
Sandec	Department for Water and Sanitation in Developing Countries, Eawag, Dübendorf, Switzerland
UN-Habitat	The United Nations Human Settlement Programme

Units & Symbols

In general, the metric system and ISO units are used throughout this report.

Detailed calculations used in the design are given in the appendices of the report. The symbols used in these calculations are explained there. Most of the units below are only relevant for those using the in-depth calculations in the appendices.

Symbol	Unit	Dimension
π	Pi (approximately 3.14)	number
A	Ampere	electric current
Ah	Ampere hours	time that a given electric current can be supplied by a battery
g	gramme	mass
J	Joule	energy
l	litre	volume
m	metre	length
mm	millimetre	length
m/s	metre per second	speed
m/s2	metre per square second	acceleration
N	Newton	force
Nm	Newton metre	torque
Pa	Pascal	pressure
Rad	Radian	angle
Rad/s	Radian per second	angular velocity
Rad/s2	Radian per square second	angular acceleration
s	second	time
V	Volt	electric force
W	Watt	power

1 Introduction

Construction of a RBC with readily available materials

As part of the STUN project, a low-tech struvite reactor has been developed in Nepal. With this reactor, phosphate can be removed from source-separated urine and used as a solid fertiliser in agriculture. The remaining process effluent is still rich in ammonium, for which several reuse options have been investigated. As one potential option for ammonium removal from the effluent, a rotating biological contactor (RBC) was designed and tested using the nitritation/anammox process. This report documents the design process, the building and testing phase of this reactor.

In the initial design phase, the type and size of the reactor were determined. Based on literature data, the expected nitrogen inflow rate for the nitritation/anammox process was calculated. With this inflow rate, the reactor size required to treat 25 litres of effluent per day, was calculated. Based on a survey of available materials and skills in Kathmandu, a number of design concepts were developed and evaluated. For the selected concept, a set of drawings and design calculations was produced, from which the reactor was built. In the main text of the report the design process is described, while the detailed calculations and technical design drawings are presented in the appendices.

After a relatively problem-free building phase, a several problems were encountered during the start-up phase. The problems ranged from the underestimation of the rotor resistance causing the belt drive to slip, to problems with the accuracy of manufacturing, to inexplicable problems with the power supply. A breakdown of the building costs of the reactor (approximately 1000 €) is also presented in this report.

At the end of the report, recommendations for improvements are given; most of those are related to issues of durability. The current reactor is designed for a limited life span (though many parts of it would function for many years without much maintenance). A similar reactor that has to function on a long-term basis, requires certain design modifications. The information provided in the report and the appendices should enable a person with a technical background to build a similar or up-scaled reactor.

2 Background

Struvite harvesting key features and STUN's starting points

2.1 The STUN project

STUN (Struvite recovery from Urine in Nepal) is a collaboration between the Swiss Federal Institute of Aquatic Science and Technology (Eawag) and UN-Habitat Nepal. During the project, a low-tech reactor for the production of struvite – a phosphorus fertilizer – from source-separated human urine has been developed (Etter et al., 2010). Publications about this research can be found on *www.eawag.ch/stun.*

2.2 Project rationale

Phosphorus (P) is a non-renewable resource that is vital as a fertilizer in agriculture. The currently known mineral resources are very limited and recent estimates showed that phosphorus demand could exceed production in only a few decades from now (Cordell et al. 2009). An increase of fertilizer demand will be particularly critical for developing countries, where the shortage of fertilizers is often responsible for insufficient food supplies (Liu et al., 2010). In recent years, the recycling of nutrients from human excreta to agriculture has steadily gained more attention (WHO, 2006). Most of the nutrients excreted by humans are found in urine: 85-90 % of nitrogen, 50-80 % of phosphorus, 80-90 % of the potassium and close to 100 % of sulfur (Larsen and Gujer, 1996). The separate collection of urine is therefore an efficient way to capture and recycle nutrients.

In Nepal and other developing countries, the promotion of sanitation based on urine-diverting dry toilets (UDDTs) has led to the emergence of a new waste stream: “source-separated urine”, which is human urine with little or no dilution and a high concentration of ammonium and a high pH value (Udert et al. 2006). In a rural setting, the urine can be applied directly to the fields; in an urban setting, where no fields are available, part of the nutrients in urine can still be recovered in the form of struvite (magnesium ammonium phosphate): when magnesium is added to urine, struvite crystals precipitate and can be filtered out of the effluent (Ronteltap, 2009; Etter et al. 2010).

The STUN project has pioneered a simple reactor (Figure 1) to precipitate struvite from urine in Nepal. However, the effluent from this reactor is still very high in nitrogen, mainly present in the form of ammonium. Possibilities for the recycling or treatment of effluent include:

- *fertigation:* drip irrigation with struvite production effluent added as N-fertilizer
- *aquaculture:* nutrient input for the production of fish and/or aquatic plants
- *conventional nitrification/denitrification* with the addition of an organic carbon source
- *co-composting* with faeces or kitchen waste
- *ammonium stripping* (Behrendt et al, 2002).

Most of these systems require significant space, maintenance, organic material or energy input.

In its current phase, STUN is researching a recently established process to treat ammonium rich waste streams: nitritation/anammox. This is a novel technology for industrialized countries, but to our knowledge, it has not been used in the developing world up to present. The nitritation/anammox has been chosen for this pilot project, because it requires only little energy and aeration and no chemical additives. The aim of setting up a nitritation/anammox reactor in Nepal is to see, whether this process can be operated with a low-cost reactor, little maintenance and under Nepalese climate conditions.

The operation of the reactor is described in a separate report (see *www.eawag.ch/stun*).

Figure 2: *The STUN struvite reactor developped in Nepal.*

2.3 Nitritation/anammox process

Nitritation/anammox is a process in which aerobic ammonium oxidizing bacteria convert part of the available ammonium to nitrite (nitritation), and anoxic ammonium oxidizing bacteria combine the produced nitrite and remaining ammonium into nitrogen gas and water. This process was first observed in wastewater treatment plants and has been researched extensively in the Netherlands and Switzerland (Kuenen, 2008; Fux et al, 2002). It is a process in which ammonium can be removed from wastewater streams in a more efficient way then with the usual nitrification/denitrification process. The input for the anammox reactor is the effluent from the struvite production process or urine. The effluent used in our experiments has a high pH value (around 9), containes high ammonium concentrations (about 2300 mg $N \cdot L^{-1}$), a high content of dissolved organic compounds (about 4500 mg $COD \cdot L^{-1}$) and low suspended solids content. In the reactor, bacteria live in a biofilm on a series of rotating discs. The aerobic ammonium oxidizing bacteria and the anammox bacteria are part of this biofilm. Another important group of bacteria in the biofilm are organo-heterotrophic bacteria, which degrade the organic compounds. Because the discs rotate, the biofilm is alternately in contact with the effluent and with the air. During the process, part of the ammonium is converted to nitrite by aerobic ammonium oxidizing bacteria. After this step, a mixture of ammonium and nitrite is available in the biofilm. This mixture is the substrate for the anammox bacteria. If sufficient oxygen is available in the reactor, nitrite oxidizing bacteria will convert some of the nitrite into nitrate. This is an unwanted process, which can be prevented by keeping the oxygen concentration in the reactor low. The start culture of bacteria used to inoculate the reactor was imported from a wastewater treatment plant in Zurich, Switzerland.

2.4 Rotating biological contactor

Rotating biological contactors (RBC) were originally developed in Germany in the late 1960's and have found many applications since then (Metcalf and Eddy, 2003). They consist of a series of parallel discs rotating on a central shaft. In most installations, the discs are submerged in the effluent for about 40 % of their surface. The shaft with the discs slowly rotates (between 1 and 5 RPM are common values). Therefore, every part of the disc is alternately submerged or in contact with the air. On the discs, a slime layer – biofilm (Figure 2) – containing bacteria develops; to increase the disc surface area, a porous or textured plastic material can be used (Vlaeminck et al. 2009).To treat source-separated urine, the reactor is inoculated with anammox rich sludge. Other bacterial cultures may be used to treat domestic wastewater. RBCs are a good option for decentralized wastewater treatment, e.g. at a hotel in the mountains. The strong points of the RBC are (Arceivala and Alesokar, 2008 & Metcalf and Eddy, 2003):

- low energy consumption
- low land requirement
- simple operation
- low maintenance (once biochemical process established)

Figure 1: *Biofilm growing on the foam coated discs of a RBC.*

3 Preliminary design phase

How available materials and skills influenced the design decisions.

3.1 Design criteria

3.1.1 General design criteria

Based on experience from nitritation/anammox research at Eawag and literature data, the following basis of design was defined:

- The reactor will be a RBC.
- Turbulences created by the rotating discs should be kept at a minimum. Excessive oxygen input promotes the growth of nitrite-oxidizing bacteria, and inhibition of anammox bacteria.
- Discs are to spin at approximately 3 RPM and to be clad with synthetic foam on both sides to increase surface area for bacteria growth.
- The rotor is to be submerged as close to 50 % as possible, so that all the disc area will be used for biofilm growth.
- To avoid corrosion, steel parts are to be avoided for the parts of the reactor, which are in contact with the effluent.

3.1.2 Nepal specific design criteria

As the reactor is to be built and used in Nepal, other limitations have to be observed. These may also apply in other developing countries:

- The reactor has to be low cost.
- Locally available materials will be used for the construction.
- The reactor has to be powered by a 12 Volt motor, due to the long periods – up to 12 hours per day – of load-shedding (power outage), and the high costs of inverter and batteries to provide 220 V during blackouts.
- As no lifting or hoisting gear is available, a maximum weight of individual parts is set at:

  - components to be handled by 1 person: 25 kg

  - components to be handled by 2 persons: 50 kg

  These maximum weights are not only motivated by health and safety concerns, but also by the knowledge that people will handle heavy items with less care and thus may damage them.

3.2 Design parameters

The required size of the reactor is mainly a function of the ammonium concentration in the urine and the volume of urine to be treated. After some tentative calculations, it was decided to build a pilot reactor that can treat 25 litres of urine per day. This is not enough to treat all the effluent from the struvite reactor, if the latter is operated on a daily basis. However it is sufficient to examine the viability of nitritation/anammox in Nepal. The number of 25 litres/day is based on the following design assumptions:

- From literature data (Windey et al, 2005), it is estimated that a fully developed anammox culture can be loaded with 1.8 to 2.0 grammes nitrogen per square metre of disc surface per day in a RBC (1.8 to 2.0 g $N \cdot m^{-2} \cdot d^{-1}$).

- The reactor influent will contain 7 grammes ammonium-N per litre (7 g $N \cdot L^{-1}$). Measurements of nitrogen in locally source-separated urine (Gantenbein and Khadka, 2009) suggest that the real concentration may be lower, probably due to ammonia volatilization.
- Using an open-celled plastic as the disc surface will increase the available surface for the bacteria. No exact data on the foam for sale in Kathmandu are available, but based on literature (Windey et al. 2005), an area multiplication factor of 3 is assumed.

For complete calculations of reactor capacity see Appendix AI.1.

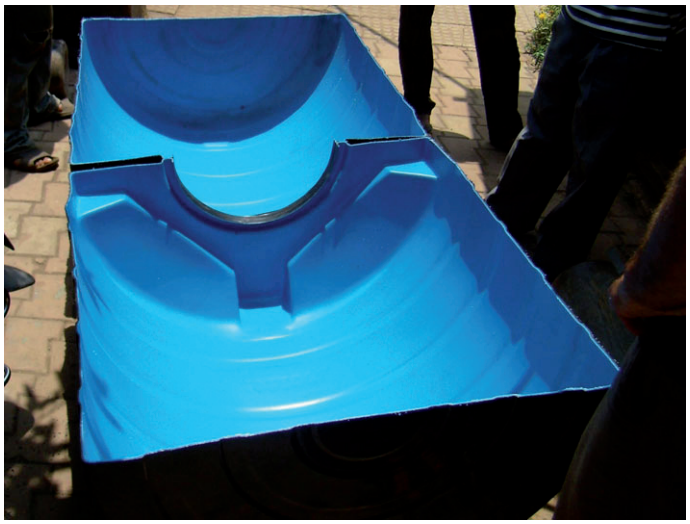

Figure 3: *A water tank being cut (top) to produce the reactor vessel (bottom).*

3.3 Material selection

A survey was made of skills (Table 1) and materials (Table 2) that were available for the reactor design in Kathmandu.

Table 1: *Skills assessment*

Skills	Description
Welding and steel works	Widely available
Plastic works	Limited to pipe fitting
Machining	Mainly limited to lathe work
Labour costs	Low
Material costs	High in comparison to labour, as many items are imported

Table 2: *Material assessment*

Item	Potential use	Description
PE water tanks	Reactor vessel	Two halves of a PE water tank (type used in urban houses) are used as a “tub” (Figure 3).
PP-R and PVC pipe	Shafts	PP-R is preferred because of its higher flexibility, strength and better chemical inertia.
Galvanized steel pipe	Shafts	Is available in a limited range of sizes with thin walls, so not very strong. More corrosion resistant than painted steel. The galvanized layer should not be damaged.
Plywood	Discs	Concerns over water ingression. May be suitable after coating with polyester resin.
Polyester fibreglass	Discs	Processed locally, but costs are high and ongoing emissions of residual styrene may influence the bacteriological process.
Soft poly-urethane foam	Biomass carrier	Is used in manufacturing outdoor gear and other applications and is widely available. Thickness: 4, 8 and 12 mm are common.
Solid round nylon bar	Bushing	Is available in 1, 2, 3, and 4 inch diameter.
Steel pipe & T- /L-bars	Frame	Widely available.
(Motor)bike and car parts	Drive & bearings	Widely available.
Building materials	Miscellaneous	Expensive as they are often imported.

3.4 Preliminary design process

The design process started with a conventional design of foam-clad discs on a central shaft. During the design process, this concept was abandoned and the reactor evolved into the current design. This paragraph is intended to review the way we proceeded from one concept to the next (see Table 3 for a comparison), and the considerations that led to our decisions.

3.4.1 Concept 1:
Foam-clad discs mounted on a central shaft

This is the common design for RBCs. The main difficulty with this design is to find a structural material for the discs that is strong enough and yet light, thin and not too expensive. Below, the strong points and weaknesses of the concept are summarized:

Strengths:

+ Central shaft to transfer weight of discs to the bearings and torque from drive along the shaft.
+ Simple design
+ "Clean" rotor design; few moving parts in the effluent and therefore not much turbulence.

Weaknesses:

- Disc structural material (to which the foam with biofilm is attached) has to be strong but thin.

  Available options: Plywood, fibreglass, and sheet metal
- Disc materials are either susceptible to corrosion or water ingression or expensive.
- All discs are permanently mounted on a central shaft. It is impossible to remove individual discs for inspection of the biofilm growth.
- The weight of all discs fitted on the shaft is too high to be handled safely without lifting gear.
- Difficult to attach discs to the steel central shaft without damaging the galvanising layer that protects it from corrosion.

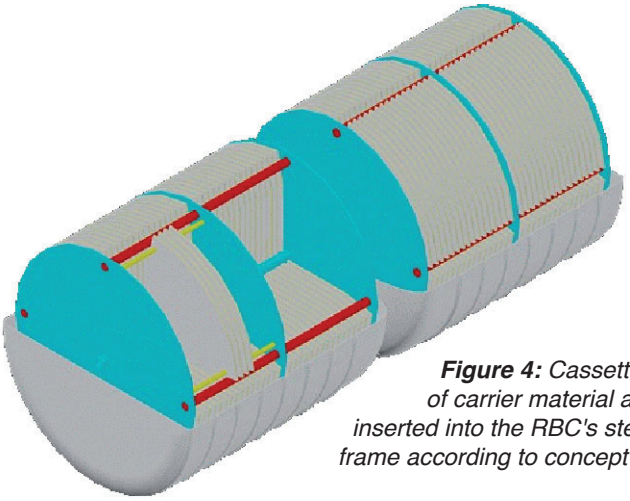

Figure 4: *Cassettes of carrier material are inserted into the RBC's steel frame according to concept 2.*

3.4.2 Concept 2:
Modules on a central shaft

To overcome the weight issue, a modular approach was explored (Figure 4). This design is closer to an industrial RBC, where the rotor consists of a steel frame on a central shaft, in which cassettes of carrier material are fitted. We designed a frame holding cassettes made out of a stack of 12 quarter-circle segments. The cassettes can then be inserted and removed for inspection.

Strengths:

+ Component weights can be reduced to manageable size.
+ It is possible to remove individual cassettes for inspection.

Weaknesses:

- Disc structural material to which the foam with biofilm is attached has to be strong yet thin (but less than for concept 1, as the segments are smaller than the complete discs).
- Segment material is susceptible to corrosion, water ingression or expensive.
- More complex design and more parts moving in effluent, which leads to more turbulence and aeration.
- The rotor overall weight is quite high, thus shaft, bearing and motor have to be sturdy.

Table 3: *Comparative chart of the reactor concept evolution.*

Component	Concept 1	Concept 2	Concept 3
disc mounted on	shaft	shaft	cage
disc material	plywood / fibreglass	plywood / fibreglass	foam
disc removal possible	no	in cassettes	individual
shaft material	galvanised steel pipe	galvanised steel pipe	PP-R
foam attached to	disc	segmented disc	rim
rotor weight	medium	heavy	light
expected turbulence	low	medium	high
price	high	highest	low

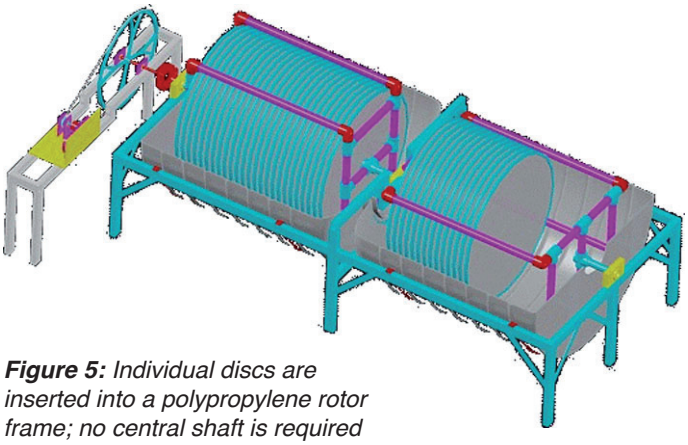

Figure 5: *Individual discs are inserted into a polypropylene rotor frame; no central shaft is required according to concept 3.*

3.4.3 Concept 3:
Flexible discs in a rotor frame

During design and evaluation of the first two concepts, it turned out that the structural material for the discs or disc segments would become a significant contribution to the overall cost of the reactor. In response to this, a new concept was developed, which is not based on sturdy discs or disc segments.

In the new concept, the discs consist of a fabric surface stretched inside a rim, which is made of plastic pipe (Figure 5). To increase the surface for biofilm growth, foam can be attached to the fabric. The tension in the fabric and the compression of the rim maintain the circular shape of the discs. In this concept, a central shaft is no longer possible, because the discs cannot have a hole in the middle. Instead, the rotor is designed as a frame or "cage" (Figure 6), in which the discs can be fitted between the bars. The discs are sufficiently flexible to deform and fit through the bars.

While assembling prototypes, we realized that it was difficult to stretch the fabric over the rim. For the second prototype we used foam circles, which are smaller than the rim. The foam has elastic loops sewn on to its edge. With these loops, the foam is stretched inside the rim. This option is assumed to be strong enough to survive for approximately 6 months, but for a more durable reactor, a different design has to be considered.

This design is quite different for other RBC designs and has the following strengths and weaknesses:

Strengths:

+ Light weight.
+ No expensive disc material.
+ Individual discs can be removed for inspection.
+ Frame and short parts of shafts can be made of PP-R pipe, which does not corrode.

Weaknesses:

- Discs are made of soft foam, which might not be very durable.
- The cage construction leads to more turbulence, so that the aeration might be too strong for nitritation/anammox

The weak points of the reactor could be detrimental for the process, therefore, we discuss them in more detail:

Low durability: Our reactor will only work for 6 months to test the nitritation/anammox process in Nepal. Based on prototypes made, we feel confident that the discs will last during the test. For a permanent reactor, other materials will be needed. The biofilm of the discs is not expected to be more than 3 mm thick. For our small discs, this will mean a maximum weight of 2 kg of wet growth per disc, which the foam should be able to support.

Turbulence and aeration: The fact that the rotor moves very slowly (3 rpm) and has a limited diameter, makes that the bars of the frame only move at 0.10 metre per second through the effluent. At this speed, not much turbulence will occur, thus aeration of the effluent should be minimal. During the experiments, this assumption was partly proven wrong, as the constant submerging and surfacing of rotor parts does cause considerable turbulences and a corresponding high level of dissolved oxygen. From observations it seems likely that the high dissolved oxygen is partly due to air transport by the foam of the discs. Air bubbles remain in the foam when it submerges and are released in the effluent. It is not possible to determine how much of the aeration is due to the foam and how much due to the rotor frame. This air transport would also occur for concept 1.

Figure 6: *The assembled polypropylene rotor carrying a prototype foam disc is tested in the reactor vessel.*

4 Detailed design phase

The components of the RBC interact to function as a machine.

4.1 Design selection

The RBC is designed according to concept 3 (see appendix AII.1). From the size calculations (section 4.2), it was determined that 48 discs of 650 mm diameter are required to treat approximately 25 litres of urine per day.

Two halves of a water tank are used as reactor vessel. Due to the shape and size of the tank, the discs are grouped in two sets of 24. The discs are in the rotor frame with 20 mm space between the discs. Small spacers prevent sideways motion of the discs. The frame is made from PP-R pipe and reinforced with steel pipes inside in critical areas. For a more detailed description of all parts see section 4.3. Figure 7 shows the completed reactor including the drive assembly, battery and charger.

4.2 Dimensioning of components

4.2.1 Power requirement

To design the drive train of the reactor, the required power has to be known first. We used simplified calculation models to determine the required torque and power to start the rotor and to keep it going.

When the RBC is turning, there is a resistance that slows the rotor down, which the motor and drive have to overcome. Once the rotor is turning at its operational speed, this resistance can be divided into two components:

a) Resistance due to friction of parts moving through the liquid (viscous resistance): Can be calculated with a simplified model based on commonly accepted formulas from fluid mechanics. According to these calculations, this is the largest component of the resistance. However, the calculation model is not very refined. Whenever assumptions are made, we use a conservative approach. As a result, the resistance calculated is probably overestimated (see appendix AI.2).

b) Resistance due to buoyancy of rotor parts: Is due to the fact that the rotor is made out of a 3-dimensional pipe frame. During the rotation, parts of the rotor are submerged in the effluent. On those submerged parts, a buoyancy force acts (see appendix AI.5). Because not every part of the rotor is submerged at the same time, the resistance due to the buoyancy varies during the rotation of the RBC. In the referred appendix, the worst case (maximum resistance) is presented.

During start-up there is an extra component:

c) Resistance due to inertia (the force required to accelerate the rotor): This resistance is caused by the energy required to accelerate a mass. The calculation of this component is based on a simple calculation of the rotor's inertia and an assumed acceleration time (see appendix AI.3).

Each resistance component above can be expressed as a torque (force required to turn the rotor). As a conservative approach, we can assume that during the final stage of the acceleration time all 3 components have their maximum value. This value is the design torque, for which the motor is selected (calculations see Appendix AI.6). With both the torque and the rotation speed defined, the required power is also calculated in this appendix.

4.2.2 Motor and gearing specification

The power and torque required fit well within the limits of most 12 volt systems, which is an advantage considering the long periods of "load-shedding" in Kathmandu. It should be noted that calculations are approximate and assumptions are conservative. The most powerful and widely available 12 volt motors are the wiper motors for car windshields. An added advantage of these is that they are mounted in one unit with a worm gear that reduces the revolving speed (RPM) of the motor significantly: The output of our motor is 38 RPM, so further gearing down is required to get to the 2 to 3 RPM that the reactor should have. Gearing down also increases the available torque. The maximum (stall) torque and free running power usage of the motor were determined by measurements with a spring balance attached to a lever on the main shaft. Based on these parameters, the requirements for the gear system could be specified (appendix AI.4).

4.2.3 Battery capacity and charger selection

With the motor's specifications known, the batteries can also be specified. The batteries need to be able to bridge the duration of blackouts with some margin, as we cannot assume that they will always be completely recharged when the periods of power supply are short.

If a continuous power supply is required, so-called deep cycle batteries are more durable than car batteries. The capacity of a battery is given in ampere-hours (Ah), i.e. the number of amperes a fully charged battery can supply over a certain duration of time before it is empty. However, if the battery is discharged deeply during every use, it will not last many load cycles. It is recommended that for normal use, the battery be never discharged for more than 30 %. Hence, 70 percent of the capacity (Ah) should remain in the battery (this is called 70 % depth of discharge)(calculations see appendix AI.4).

The charger needs to be automatic, i.e. it can be permanently connected and will measure when the battery needs to be charged. Home chargers for car batteries are not suitable because they do not have this function. Two different automatic types are available: electrically controlled and electronically controlled. The latter ones are more reliable. In Nepal, the two types do not differ in price, which is why we selected an electronically controlled charger.

Figure 7: *The completed RBC with its drive unit on the right side.*

4.3 Design of components

4.3.1 Discs

The discs are made of a plastic rim (16 mm HDPE-pipe) with a soft-foam centre (see Figure 8 and appendix AII.2). The foam is hemmed with a strong band of fabric, also used for backpack straps. Eight loops of elastic band are sewn to the hem of the foam discs. The rim pipe is looped through the eight elastic loops and then bent to a full circle. The ends are connected by a wooden peg inside the pipe.

These discs are flexible enough to be inserted into the rotor frame. Once inside, they resume a round shape and remain fixed in place. The elastic loops stretch the foam tightly. Spacers cut from a 40 mm PP-R pipe hold the foam discs equally spaced in the rotor frame (for details see inset Figure 8).

The foam has to be stretched carefully for maximum tightness without over stretching and tearing it. For a reactor, which is to be operated for several years, the foam should not be a structural part of the discs. Adding a middle layer of fine plastic mesh (e.g. mosquito netting), onto which the foam is attached, could improve durability. If the middle layer is slightly flexible, the loops can be replaced with non-elastic material, which does not slacken over time.

4.3.2 Rotor frame

The discs are fitted into the rotor frame (appendix AII.3). The frame is made out of PP-R plastic pipes and fittings. They are coupled by melting the ends and sockets and joined together while still molten (Figure 9). During the final stages of the rotor assembly, a number of connections is made simultaneously. For these connections, bolts are used, because it is not practical to weld them simultaneously. To avoid excessive deformation of the rotor, steel pipes are inserted into the longest plastic pipes.

No detailed strength calculations for the rotor were made due to time constraints and missing data on the piep material's mechanical properties. Instead of calculations, we relied on prototypes constructed for various parts. If a larger version of the reactor will be built, better strength calculations will have to be made. Here are some critical points, which have to be considered:

- On large discs, the extra weight of the biofilm has to be considered, when choosing the stability of the rotor and bearings.
- The torque from the motor has to be transferred through the three-dimensional pipe structure. As size increases, the required power and the resulting torsion will increase.
- If stiffer materials are used, the bearings and the running surfaces on the shafts have to be aligned very accurately to avoid excessive abrasion and fatigue due to shaft bending.

Figure 8: *The foam discs are ready for assembly (above). PP-R spacers hold the discs equally spaced on the rotor frame (inset).*

Figure 9: *During the rotor frame assembly, the parts are fitted (above) and subsequently welded using a hot plate (inset).*

4.3.3 Bearings

To avoid corrosion and allow simple manufacturing, the bearings are plastic plane bearings (Figure 10) instead of metal ball bearings (appendix AII.4). In plane bearings, a smooth surface on the shaft runs in a machined bush, here made out of nylon. No lubrication is necessary, because the rotation is slow and bush and axis are made of plastic. The bushes are fixed to the frame by clamping them into wooden blocks. The alignment of the bearing surfaces on the shaft requires high accuracy.

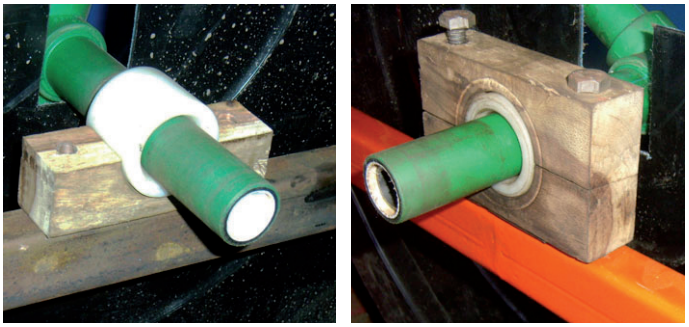

Figure 10: *Nylon bush (left) clamped in a wooden block (right).*

4.3.4 Frame and tank

The reactor vessel is made of a plastic water tank cut in halves. Steel is not a good choice for source-separated urine because of corrosion, but might be suitable for other types of wastewater. The entire reactor is supported by a simple metal frame (Figure 11; appendix AII.5), which should be painted with high quality paint to prevent corrosion by urine splashes.

Figure 11: *The reactor frame under construction.*

4.3.5 Drive system

The drive system (Figure 12; Appendix AII.6) is attached to the rest of the reactor with a flexible coupling, which allows using different types of motors. For our reactor, we used a windshield wiper motor of a Suzuki Maruti, a common type of taxi in Nepal. The motor unit includes a gearing system that makes the output shaft spin at 38 RPM. A belt drive system is used to gear down to 3 RPM (gearing ratio of about 1:13). The large pulley was taken from a foot-powered sewing machine. The smaller pulley was dimensioned so the gearing ratio suits and was produced specifically for this reactor. The advantages of the belt drive are:

- simpler to build than cogwheels
- less sensitive to misalignments
- If the rotor blocks, belt slip will prevent damage to the motor.
- Because the price for the large pulley is low, the entire drive system can be built at a low price compared to a gearbox.

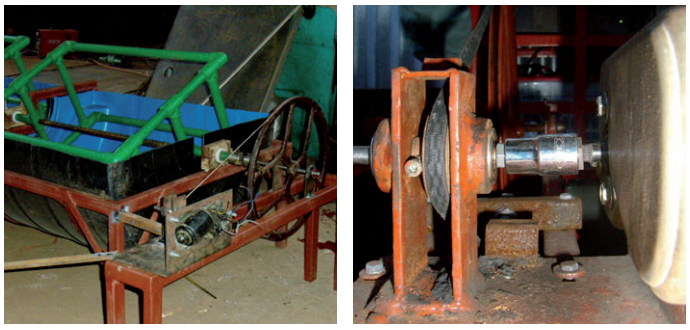

Figure 12: *Drive (left) and coupling from motor to pulley (right).*

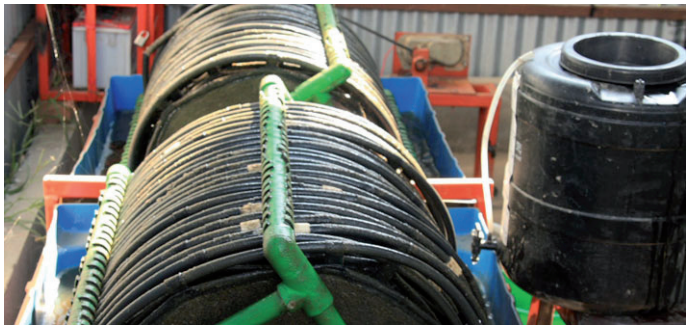

Figure 13: *Drive (left) and coupling from motor to pulley (right).*

4.3.6 Reactor influent tank

After a functional nitritation/anammox culture is established, about 25 litres of influent per day are required to operate the reactor. This influent should be added to the reactor gradually. As dosing pumps are not available, a system with a header tank will be used. The tank is filled with the effluent from the struvite reactor on a daily basis. Through a tap in the header tank, the influent drips slowly into the reactor (Figure 13; appendix AII.7).

4.3.7 Battery cage

As the research facility is not burglar proof, the expensive electric components (e.g. battery, charger and voltage controller) are locked in a steel cage (Figure 14; appendix AII.8). This cage is welded to the main construction of the lab to prevent theft.

Figure 14: *Battery and charger are locked up in metal cage.*

5 Experiences from building and testing

As the RBC takes shape, the design has to prove its functionality.

5.1 Experience with contractors

The reactor is not a highly complicated machine, but the construction company needs to be skilled in welding, plumbing and machining (primarily with a lathe; see Figure 15). It pays to select a company that is used to working from construction drawings and has built machines incorporating bearings and drive systems before.

Having good drawings with a lot of information proved to be very helpful. Our experience was that the drawings were easily understood and used well, which saved a lot of time for construction supervision.

For the drive system, the drawings were not very detailed, as we assumed the production company would have considerable input and additional ideas. This assumption proved to be partially correct, but the company would not implement their ideas without consulting the engineering team. For future projects, it will be best to produce some concept drawings, discuss these with the production team and then produce detailed drawings for the assembly of the drive.

We found that in order to keep the process moving, we had to pay daily visits to the construction company. Once a working relationship was established, they would ask us to be there a whole day, at times when work on a new item was started and during final assembly of the machine. We did have to support the company with the work planning in order to convince the coordinators to make several different components simultaneously, in order to limit the overall construction time.

In the end, we were very impressed by the quality of the work, especially considering the relatively simple tools, which were used.

Figure 15: *Precise machining of the wooden block holding the nylon bush of the RBC.*

5.2 Experience during testing and commissioning

The drawings in the appendices represent the final working machine. Some design decisions that were made, did not work well, but the implications of changing these are too big to tackle within our project. In chapter 6, recommendations are given to improve the design.

Below, in Table 4, some problems and solutions are discussed. The solutions in this table have been incorporated in the design drawings in the appendices.

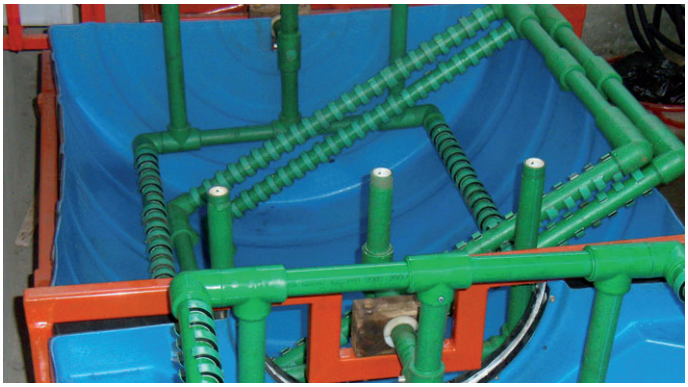

Figure 16: *The rotor is waterproofed with silicon sealant.*

Table 4: *Problems encountered during start-up and solutions*

Problem	Description	Solution
Undersized discs	Manufacturing problem: the company, which manufactured the discs, did not work accurately enough producing the rims. As a result, some discs did not stay in place, once fitted in the rotor.	Make new rims for the discs. As slightly different material was used, this resulted in fractured rims (described below).
Fractured rims	The HDPE pipe used to replace the non-fitting discs was smaller in diameter and had a thinner wall. As a result, the pipes were not strong enough and started to fracture at the location of the wooden peg.	We recommend that the connection of the HDPE pipe be made with a sleeve over the joint rather then with a wooden peg inside it (see drawing appendix H).
Water in rotors and discs	Most of the connections in the rotor are welded and thus water tight. The few bolted connections are prone to water intrusion, resulting in higher friction for the spin of the rotor.	Reassemble the rotor with silicon seal in the joints that are not welded (Figure 16).
Slipping transmis-sion belt	During the initial design, the resistance due to buoyancy was omitted. The obtained values suggested that the required torque for the drive train would be low enough to be transmitted using a normal leather belt (as used on foot-powered sewing machines). In practice, the belt slipped despite various experiments to tighten it.	Replace the leather belt with a rubber V-belt. The small pulley had to be refitted to the new belt. However, the V-belt does not fit well on the larger pulley, so there is significant wear. But it is expected to withstand the wear for the duration of the experiments.
Fluctuating rotor speed	Apart from the problems with the transmission, the buoyancy also caused the motor and the rotor to turn very irregularly; the rotor was alternately slowed down or accelerated by the buoyancy force. The belt drive and the flexibility in the coupling and pipes increased the irregularities further.	The rotor was cut in half at the central shaft and the rotor halves were rejoined at a 90-degree angle. In addition to solving the problem, this reduced loads on the belt drive and motor.
Wear in motor gears	The wiper motor features a built-in gear system: from the worm gear, a short shaft leads out of the gearing house, where a short arm is mounted. Originally this connected to a lever on the driving pulley shaft. Initially chosen to avoid precise machining and ensuing alignment problems, this arrangement expedites wear on the gear parts.	A new design with a straight coupling is now functioning well, without causing problems for the motor gear.
Malfunction in battery charger	During the initial phase, breakdowns of battery charger caused delays. The precise cause of the problems was never found.	Install a peak voltage suppressor in the system

5.3 Building costs

5.3.1 Overview of reactor building costs

The table of costs is presented here (Table 5). The first is subdivided in groups, which represent the blocks sourced-out to different suppliers. The latter deals with items related to the battery cage, a metal cage welded to the lab structure to prevent theft of battery and other electronic equipment. All prices in the table include 13% VAT, they are both given in Nepalese Rupees (NRs) and Euro, the exchange rate during construction was about 96 NRs to 1 €.

Table 5: *RBC cost breakdown*

Item	Cost	Cost	Group total	Estimated labour cost:
Units	*NRs*	*€*	*€*	*€*
Discs:			*133*	*53*
Discs labour and foam	9325	97		
HPDE pipe for discs	1615	17		
Wooden pegs for discs	1800	19		
Reactor main structure:			*527*	*211*
PE water tank	4500	47		
Metal support frame for reactor	13560	141		
Rotor structure and bearings	22600	235		
Drive unit and coupling	9040	94		
Silicon	250	3		
V-belt	600	6		
Electronic equipment:			*249*	*-*
Battery	9040	94		
Battery charger	11300	118		
Wiper motor	1850	19		
Electric wiring etc.	1200	13		
Voltage controller	500	5		
Miscellaneous items:			*30*	*-*
Transportation of reactor	600	6		
Influent header tank	1800	19		
Influent and effluent connection hoses	500	5		
Auxiliary items:			*60*	*24*
Battery cage, steel structure	4520	47		
Plywood cover for battery cage	150	2		
Anchoring battery cage to lab structure	600	6		
Locks for battery cage	500	5		
Total:	**95850**	**998**		**288**

5.3.2 Further notes about the cost overview

All items were contracted on a lump sum basis, therefore no accurate breakdown of material cost versus labour costs can be made. However, based on knowledge of local material and labour costs, it is estimated that both for the discs and for the construction work, a split of 40 % labour and 60 % materials is realistic. The group 'electrical equipment' does not contain labour, because all wiring was done by the project team. If this is done by a Nepali tradesman, it will have cost approximately 700 NRs.

Design and engineering was done by the project team, so no costs for this are included. If design and engineering are subcontracted (which is difficult, because no mechanical engineering services are available), it would add significantly to the costs. The engineering costs are estimated at about 70,000 NRs, which would still exclude project management by the project team.

5.3.3 Costs related to modifications and repairs

As documented in paragraph 4.2, several repairs and modifications have been made to the reactor during the start-up phase. Related costs are presented in Table 6:

As can be seen from this table, the costs related to modifications and repairs are minor. However, they were time consuming for the project team.

Table 6: *RBC repair costs*

Item	Cost	Cost
Units	*Nrs*	*€*
HPDE pipe for disc replacements	500	5
Glue and sockets for repairing discs	650	7
Wiper motor (second hand)	700	7
New pulley for V-belt	500	5
Tools for repairs	1000	10
Total:	**3350**	**35**

6 Outlook and possibilities for improvements

After a period of problem solving and modifications, the RBC works well, which proves that this type of reactor can be constructed in Nepal with locally available material. A very interesting further research would be to compare the building and operation and maintenance costs of a full-scale reactor for the treatment of mixed wastewater, in comparison to a constructed wetland.

The current reactor is only intended for a limited service life, though most of its components could function for several years with little maintenance. Parts of the reactor, which may have low durability:

- Motor and built-on gears
- V-belt
- Discs

The wiper motor and gear are not intended for a very long usage time. With the new coupling, the gear on the motor no longer breaks down. However, since the replacement, one motor has broken down. A more durable, more powerful motor is needed to ensure continuous operation.

As the large pulley is not designed for the V-belt, it leads to excessive wear on the belt. A larger size V-belt is likely to solve this problem. Even if a better fitting belt is found, it will have to be replaced occasionally as part of regular maintenance.

The discs also encounter durability issues; the foam and elastic band used will not last in a longterm application. In section 3.3.1, some possible improvements are suggested. There have been problems with the discs breaking at the wooden peg that is supposed to keep them together. A better coupling with a sleeve over the joint, rather than a peg inside, is presented in appendix AII.2.

Another solution to avoid the described problems with the discs, is to build a completely different rotor. This would be a rotor according to the more usual concept 1 discussed in paragraph 3.1. A concept drawing of this type of rotor is presented in appendix O. With this design, the weight of the rotor will increase quickly. As indicated on the drawing, the current size of shaft and bearings can only be maintained if the total weight of the rotor can be kept below approximately 50 kg.

Opting for this type of rotor would solve a lot of potential durability issues and, at the same time, lower the resistance of the rotor, because the component due to buoyancy could be excluded. The two drawbacks are:

- Higher building costs (estimated at NRs 21,000 – 200 Euro – with plywood discs).
- High weight of rotor, this would cause some problems during assembly.

This report with the appendices contains most of the information and methodologies to design an up-scaled version of the RBC. The items, which are not covered, include strength calculations, as they were not pursued in detail. For an up-scaled version, structural analyses will be required, because weight and forces will increase exponentially with size.

Acknowledgements

The authors would like to express their thankfulness:

- to UN-HABITAT Nepal for the institutional support received during the research in Nepal.
- to the Kuleshwor Secondary School for hosting the RBC experiments and contributing urine input.
- to the village of Siddhipur and Jiban Maharjan who regularly contributed urine for the RBC tests.
- to the Eawag lab team for the valuable inputs concerning the anammox process.
- to Power Tech Pvt. Ltd. in Lagankhel, Lalitpur for the high precision construction of the RBC.
- to the Environmental and Public Health Organization (ENPHO) for the assistance on analysis.
- to the wastewater treatment plant Werdhölzli in Zurich, Switzerland for the inoculation culture.
- to the Aqautic Ecology Centre at Kathmandu University for laboratory support.
- to Elizabeth Tilley and Christian Zurbrügg for the project supervision.
- to Raju Khadka, Roman Meyer, and Marco Kunz for their hard work during the test phase.
- The Symphasis Foundation for financial support.

7 References

Further readings

More information on the project and manuals for operation please look on: *www.eawag.ch/stun*

You may find following documents on the website:

- Low-cost Rotating Biological Contactor: Operation and Maintenance Manual
- Low-cost Struvite Recovery: Construction Manual
- Low-cost Struvite Recovery: Operation and Maintenance Manual

Other reports about the STUN project, on the production and economy of struvite, the re-use of effluent and the construction of a struvite reactor.

For more in-depth information of the nitritatation/ anammox process, please refer to the publications to the right.

Arceivala, S.J., Alosekar, S.R., (2008), Wastewater treatment for pollution control and reuse, Third edition, Tata McGraw-Hill Publishing Company Limited, New Delhi, India.

Behrendt, J., Arevalo. E., Gulyas. H., Niedereste-Hollenberg. J., Niemiec. A., Zhou. J., Otterpohl. R., (2002): Production of value added products from separately collected urine. Water Science & technology, Vol 46, pp 341-346.

Cordell, D., Drangert, J.O., White, S., (2009): The story of phosphorus: Global food security and food for thought. Global Environmental Change 19 (2), 292-305.

Etter, B., Tilley E., Khadka R., Udert K.M., Low-cost struvite production using source-separated urine in Nepal, Water Research (2010), doi:10.1016/j.watres.2010.10.007

Fux C., Boehler M., Huber P., Brunner I., Siegrist H. (2002): Biological treatment of ammonium-rich wastewater by partial nitration and subsequent anaerobic ammonium oxidation (anammox) in a pilot plant. Journal of biotechnology 99. 295-306

Kuenen, J.G. (2008): Anammox bacteria: from discovery to application. Nature Reviews Microbiology Volume 6. 320-326.

Larsen, T.A., Gujer, W. (1996) Separate management of anthropogenic nutrient solutions (human urine). Water Science and Technology 34 (3-4 -4 pt 2), 87-94.

Liu, J., You, L., Amini, M., et al. (2010). A high-resolution assessment on global nitrogen flows in cropland. Proceedings of the National Academy of Science 107 (17), 8035-8040.

Metcalf & Eddy (ed.) (2003): Wastewater engineering: treatment and reuse. 4th edition/revised. Tata McGraw-Hill Publishing Company Limited, New Delhi, India

Ronteltap M. (2009): Manuscript. Phosphorus recovery from source-separated urine through the precipitation of struvite, A dissertation for the Degree of Doctor of Technical Sciences. Swiss federal institute of technology, Zurich, Switzerland.

Udert, K.M., Larsen, T.A., Gujer, W. (2006). Fate of major compounds in source-separated urine. Water Science and Technology 54 (11-12), 413-420.

Udert, K.M., Kind, E., Teunissen, M., Jenni, S., Larsen, T.A. (2008). Effect of heterotrophic growth on nitritation/anammox in a single sequencing batch reactor. Water Science and Technology 58 (2), 277-284.

WHO (2006) Guidelines for the safe use of wastewater, excreta and greywater. World Health Organization, Geneva.

Vlaeminck, S.E., Terada, A., Smets, B.F., et al. (2009). Nitrogen removal from digested black water by one-stage partial nitritation and anammox. Environmental Science and Technology 43 (13), 5035-5041.

Windey K., De BO I., Verstreate W., (2005): Oxygen-limited autotrophic nitrification-denitrfication (OLAND) in a rotation biological contactor treating high-salinity wastewater. Water Research 39. 4512-4520

Appendix I Calculation Notes

AI.1 Calculation note: *Calculations to determine reactor size*

AI.1.1 Introduction

This calculation note describes the calculations to determine the size of the anammox RBC as a function of the loading rate. The calculations are based on assumptions regarding the amount of ammonium in the wastewater and the effectiveness of a rotating biological contactor (RBC) using the anammox process. After completion of the experiments, the final nitrogen loading and removal rates will be determined.

AI.1.2 Conclusions

Based on the predicted loading rate and nitrogen inflow, the reactor should have 48 discs of 650 mm diameter, made out of 8 mm thick PU foam to be able to receive 25 $L \cdot d^{-1}$ of influent.

AI.1.3 References

Windey K., De Bo I., Verstraete W., (2005): Oxygen-limited autothropic nitrification-denitrification (OLAND) in a rotation biological contactor treating high-salinity wastewater. WatRes 39, 4512-4520

AI.1.4 Assumptions and calculation input

The reactor will treat effluent from a struvite reactor. This effluent is source-separated human urine, from which phosphorus has been recovered. Based on commonly accepted values, the nitrogen content is assumed to be 7000 $mg \cdot L^{-1}$ mainly in the form of ammonium. As will be discussed in more detail below on the basis of figures from other research (Windey, 2005), it is assumed that the anammox culture can degrade 1.8 g $N \cdot m^{-2} \cdot d^{-1}$. A daily influx of 25 $L \cdot d^{-1}$ of effluent from the struvite reactor was assumed a good target for this pilot reactor. It is big enough for the research to produce accurate field results and the costs for the reactor will remain within the research budget. The discs will be clad with a layer of soft polyurethane foam, the exact properties (e.g. cell size) of which are not known. Based on comparison with other foam types, it is assumed that the foam has an available surface area for bacteria growth of 3 times the surface area of the disc (Windey et al., 2005).

AI.1.5 Estimation of loading rate

For the purpose of these calculations, the loading rate is defined as: the maximum amount of nitrogen per day per square metre of disc, which results in the maximum nitrogen removal (in mg $N \cdot L^{-1} \cdot d^{-1}$). Windey et al. (2005) published experiments with nitritation/anammox treatment of highly saline wastewater. In comparison, the wastewater we will be treating has a lower salinity. If the salt content is the main factor that influences the nitrogen removal, then using the loading rate of Windey et al. (2005) will result in conservative dimensioning.

The loading rate is calculated as follows:

1) Volumetric loading rate according to Windey et al, 2004:

$$BV = 725\ mg\ N \cdot L^{-1} \cdot d^{-1} \approx BV = 725\ g\ N \cdot m^{-3} \cdot d^{-1}$$

2) Calculation of specific area of "Windey reactor":

$$a = A_{discs} / V_{reactor} \qquad \textit{(Formula 1.1)}$$

With: a = Specific area (m^{-1})
A_{discs} = Area of discs for biofilm growth (m^2)
Note: this is the internal surface area of the foam.
$V_{reactor}$ = Water volume in reactor (m^3)

3) Area specific loading rate:

$$B_A = B_V / a \qquad \textit{(Formula 1.2)}$$

With: B_A = Loading rate per area of disc ($g \cdot m^{-2} \cdot d^{-1}$)
B_V = Loading rate per volume of reactor ($g \cdot m^{-3} \cdot d^{-1}$)

For this reactor: $B_A = 725 / 400 = 1.8\ g \cdot m^{-2} \cdot d^{-1}$

AI.1.6 Calculation of nitrogen inflow and disc number

In this section, the formulas used to dimension the reactor are given. Attached is the worksheet with the values for our design.

The ammonium inflow load is the inflow multiplied by the concentration of ammonium in the influent.

$$\Phi_N = Q \cdot S_{NH4} \qquad \textit{(Formula 1.3)}$$

With: Φ_N = Ammonium load ($g \cdot d^{-1}$)
Q = Inflow ($L \cdot d^{-1}$)
S_{NH4} = ammonium concentration in influent ($g \cdot L^{-1}$)

Based on formula 1.3, the required surface area for growing the cultures can be calculated:

$$A_{biofilm} = \Phi_N / B_A \qquad \textit{(Formula 1.4)}$$

With: $A_{biofilm}$ = Surface area required for biofilm (m^2)

As is stated above, it is assumed that the PU foam of the discs results in an area multiplication factor of 3. Thus, the area available for bacterial growth is 3 times higher than the disc area. Therefore the required disc area:

$$A_D = A_{biofilm} / f_A \qquad \textit{(Formula 1.5)}$$

With: A_D = Total required disc area (m^2)
f_A = Area multiplication factor (-)
$A_{biofilm}$ = Surface area required for biofilm (m^2)

The disc area is a function of the size of the individual discs and the total number of discs. In our reactor design, we tried various combinations until a solution was found that fitted the water tank that will be our reactor vessel (formula 1.6). The factor 2 in the formula is required because both sides of the disc will be exposed to the liquid:

$$n_{discs} = A_D / (\pi / 4 \cdot D^2 \cdot 2) \qquad \textit{(Formula 1.6)}$$

With: n_{discs} = Required number of discs (-)
A_D = Total required disc area (m^2)
D = Disc diameter (m)

Calculations to determine reactor size

Parameter	Value	Unit	Notes
Influent nitrogen concentration	7000	$gN \cdot m^{-3}$	(conservative, some nitrogen may evaporate during handling)
Volume to be treated	0.025	$m^3 \cdot d^{-1}$	
Nitrogen input	171.5	$g\ N \cdot d^{-1}$	
Nitrogen load per area	1.8	$g\ N \cdot m^{-2} \cdot d^{-1}$	Based on data from: Windey et al. (2005)
Required surface area for bacteria	95	m^2	
Disc diameter	0.65	m	
Disc surface area (one side)	0.33	m^2	
Req. number of discs.	144	-	
Area multiplication factor for foam	3	-	
Req. number of discs with foam	48	-	
Actual number of discs	48	-	
Disc thickness	8	mm	
Total volume to fluid level	362	L	
Submerged volume of discs	51	L	
Fluid volume	311	L	
Specific area	307	m^{-1}	
Volumetric loading rate	552	$g\ N \cdot m^{-3} \cdot d^{-1}$	
Hydraulic retention time	12.7	d	

AI.2 Calculation note: *Viscous resistance of rotor*

AI.2.1 Introduction

The aim of this calculation note is to describe the model used to determine the viscous resistance acting on the rotor when turning in the effluent. In the main text, the used formulas and the concept are given. In the attached calculation sheet, the calculated values for the test reactor are given.

To allow for a relatively simple calculation to be made, some assumptions have been made to simplify the model:

1. The physical properties of the urine are the same as the physical properties of water at 20°C.
2. Because of the slow speed, the disc movement does not produce any waves. Thus, the resistance is solely due to friction.
3. As there are no waves, there is also no interference between the resistance of the discs. As a result, the total resistance of the discs can be calculated by multiplying the resistance of one disc by the number of discs.
4. The resistance of the disc is calculated with formulas from fluid dynamics describing the behaviour of rectangular plates. The assumption is that the resistance of a disc is approximately equal the resistance of a rectangular plate with an equal area that is moving (linear) through a fluid at a speed equal to the tangential speed of the edge of the discs in the rotor.
5. The resistance of the rotor structure is calculated as the resistance of cylinders moving through a fluid. No added resistance due to interference with other parts is taken into account.

AI.2.2 Conclusion

The calculation model chosen is not quite representative of the discs, but it should be conservative (overestimating drag) in most respects. There are some uncertainties because of the low Reynolds number, at which the fluid interaction occurs and due to the unspecified surface roughness. The calculations should be accurate enough to give an indication of the friction resistance.

AI.2.3 References

[1] The calculation model is based on widely accepted mechanics and fluid dynamics formulas. These formulas can be found in the general domain.

[2] The input figures are based on STUN drawing 01-100-01 “Arrangement Anammox reactor” and referenced drawings.

AI.2.4 Calculation model for the resistance of 1 disc

The resistance of one disc can be calculated with some simple fluid dynamics formulas, if some assumptions are made to simplify the calculation model. As the rotation speed of the discs is very low, no waves generated by the motion of the discs are expected. If there are no waves, then there is also no energy lost in making waves. This means that the resistance of the discs moving through the fluid is completely due to friction.

The discs are assumed to be submerged for 50%. This results in a wetted surface area (area in contact with fluid) per disc of:

$$S_d = \pi/4 \cdot D^2 \qquad \textit{Formula (2.1)}$$

with: S_d = *wet surface area of disc* (m^2)
D = *diameter of disc (m)*

Calculations for the disc's resistance are based on an equivalent rectangle with the same area as the submerged part of the disc and a length equal to the diameter of the disc (Figure 17).

$$L = D \qquad \textit{(Formula 2.2)}$$

with: L = *Length of equivalent rectangle (m)*
D = *diameter of disc (m)*

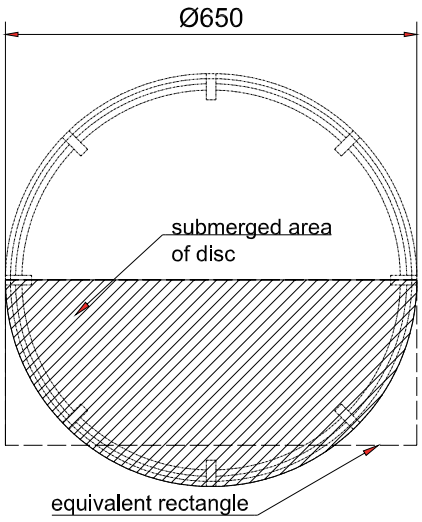

Figure 17: *Submerged part of the disc and equivalent rectangle.*

One of the main parameters in determining viscous resistance is the Reynolds number:

$$R_e = V \cdot L / v \qquad \textit{(Formula 2.3)}$$

With: R_e = *Reynolds number (-)*
L = *Length of equivalent rectangle (m)*
V = *Tangential speed of disc edge in fluid* ($m \cdot s^{-1}$)
v = *Kinematic velocity* ($m^2 \cdot s^{-1}$)

Disc edge tangential speed (V):

$$V = c / t \qquad \textit{(Formula 2.4)}$$

With: c = *Circumference of disc (m)*
t = *Rotation time (s)*
(t = 60 / RPM)
RPM = Disc rotations per minute

Kinematic viscosity (v):

$$v = \mu / \rho \qquad \textit{(Formula 2.5)}$$

at 20°C: density of liquid: $\rho = 998.5$ ($kg \cdot m^{-3}$)
viscosity of liquid: $\mu = 1.002$ (*mPa·s*)

For our reactor design, the Reynolds number is: 6.51*104. This is a very low number compared to Reynolds numbers found in fluid dynamics literature. The reasons for this are the low length and more importantly the very low speed of the disc in the fluid.

Normally, for such a low Reynolds number, one would expect the flow around the discs to be laminar and calculate the viscous resistance with the “Blasius” formula. However, the surface of the discs is very rough, so it is assumed that turbulences are generated and the boundary layer does not remain laminar. Therefore, the resistance coefficient is calculated according to the “Prandtl and von Karman” formula (2.7).

Resistance coefficient according Prandtl and von Karman:

$$c_f = 0.074 \cdot R_e^{-0.2} \qquad \text{(Formula 2.6)}$$

With: c_f = Friction coefficient (-)
R_e = Reynolds number (-)

Viscous resistance of one disc:

$$F_f = 1/2 \cdot \rho \cdot V^2 \cdot S_d \cdot c_f \qquad \text{(Formula 2.7)}$$

With: F_f= Viscous resistance of one disc (N)
All other parameters as defined above

AI.2.5 Summation of resistance due to disc drag

The total viscous resistance of the discs is assumed to be the resistance of one disc multiplied by the number of discs. An additional contingency factor takes into account surface roughness and other effects such as interferences not cover by the calculation model.

$$R_d = F_f \cdot n \cdot f_r \qquad \text{(Formula 2.8)}$$

With: R_d = Total resistance of discs (N)
F_f = Viscous resistance of one disc (N)
n = Number of discs (-)
f_r = roughness addition factor (1.25) (-)

AI.2.6 Resistance of rotor pipes

The rotor pipes also move through the effluent and therefore also contribute to the resistance of the rotor. The resistance of the pipes is, among other things, dependent on the projected area moving through the liquid (Figure 18). This area is greatest when the rotor is in a position with 4 retaining bars in the effluent. The resistance of the transverse pipes in the rotor is neglected in this model, because the speeds are low and for this size reactor the total resistance is small. This is deemed an acceptable omission.

$$R_f = 1/2 \cdot \rho \cdot V^2 \cdot A \cdot C_d \qquad \text{(Formula 2.9)}$$

With: R_f= Viscous resistance of frame (N)
ρ = Density of water at 200C ($kg \cdot m^{-3}$)
V = Tangential speed of disc edge in fluid (see above) ($m \cdot s^{-1}$)
A = Frontal area of frame pipes in effluent (m)
C_d = Drag coefficient; 0.47 for cylinder (-)

Frontal area of frame pipes:

$$A = l_p \cdot n_p \cdot d \qquad \text{(Formula 2.10)}$$

With: l_p= Immersed length of one retaining bar (m)
n_p = number of retaining bars in fluid at once (-)
d = diameter of pipes (m)

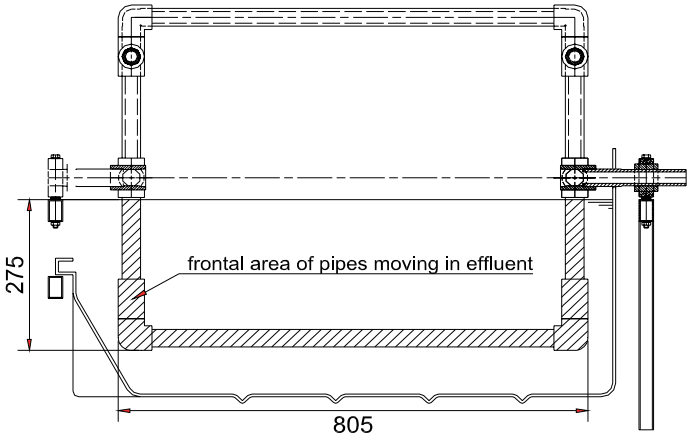

Figure 18: *Frontal area of pipes moving in the liquid.*

AI.2.7 Total resistance and power required

The total resistance of the rotor and discs is the sum of the partial resistances calculated above.

$$R_t = R_d + R_f \qquad \text{(Formula 2.11)}$$

With: R_t = Total resistance of rotor (N)
R_d = Viscous resistance of discs, see above (N)
R_f = Viscous resistance of frame, see above (N)

The resistance calculated above is valid for the rotor moving in a linear motion. To calculate the power required for rotational motion, the force has to be redefined as a torque. To be conservative, it is assumed that the complete force has its point of application on the rim of the discs (figure 19). The torque required to overcome friction is thus defined as:

$$T_f = R_t \cdot D / 2 \qquad \text{(Formula 2.12)}$$

With: T_f = Torque required to overcome friction (Nm)
R_t = Total resistance of rotor (N)
D = Diameter of discs (m)

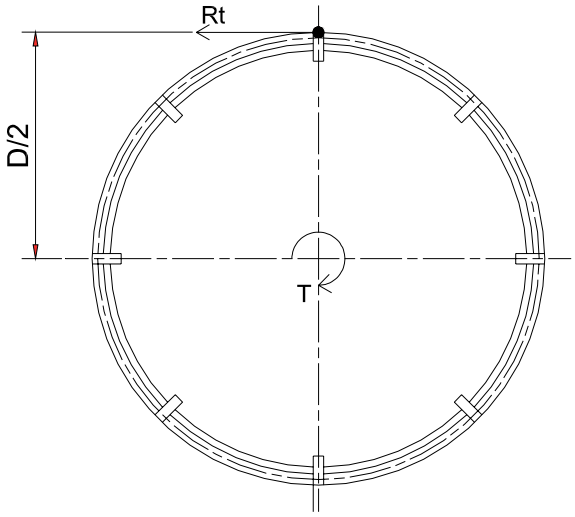

Figure 19: *Total force (Rt) acting on the rim of the disc.*

Viscous resistance of rotor

Parameter	Value	Unit	Notes
Diameter of rotor	0.65	m	
Circumference of rotor	2.04	m	
RPM	3	rpm	
Tangential speed of disc edge	0.102	m·s	
Wet surface area of one disc	0.332	m^2	
Length of equivalent rectangle	0.640	m	
Height or equivalent rectangle	0.259	m	
Viscosity of water	1.0020	mPa·s	at 20 °C
Viscosity of water	1.002E-03	Pa·s	at 20 °C
Density of water	998.5	$kg \cdot m^{-3}$	at 20 °C
Kinematic viscosity of water	1.004E-06	$m^2 \cdot s^{-1}$	at 20 °C
Reynolds number	6.512E+04	-	
P & Von K resistance coefficient	0.00806	-	
Resistance of one equivalent square	0.014	N	
Roughness addition	25	%	
Resistance of one disc	0.017	N	
Number of discs on rotor	48	-	
Total resistance against rotation due to fluid	0.84	N	
Number of retaining bars in fluid	4	-	
Length of retaining bar	1.36	m	
Diameter of retaining bars	0.032	m	
Frontal area of retaining bars	0.17	m^2	
Drag coefficient cylinder	0.47	-	
Drag of retaining bars	0.42	N	
Torque required to overcome friction	3.88	Nm	

AI.3 Calculation note: *Torque required to start the rotor*

AI.3.1 Introduction

The aim of this calculation note is to describe the calculations made to determine the torque that the drive has to develop to accelerate the rotor of the reactor from standstill to the operating speed. To determine this starting torque, the inertia of the rotor has to be calculated. This inertia is the resistance of the rotor against a change of speed. It is a function of the mass of the rotor and of the way the mass is distributed in relation to the shaft.

AI.3.2 Conclusions

Because the diameter of the rotor is relatively small, and the mass, including biofilm, is also relatively small, the torque required to accelerate the rotor is about 1.0 Nm.

AI.3.3 References

[1] The calculation model is based on widely accepted engineering mechanics formulas. These formulas can be found in the general domain.

[2] The input figures are based on STUN drawing 01-100-01 “Arrangement Anammox reactor” and subsequently referenced drawings.

AI.3.4 Calculation input and assumptions

Since the mass of the rotor is the main variable in this calculation, it has to be determined first. It is assumed that the reactor needs to be able to start turning when there is already a layer of biofilm on the discs. Further, it is assumed that the mass of the rotor is evenly distributed throughout the rotor.

It should be noted that the rotor and biomass are partly submerged in the effluent. This means the weight loading on the shaft and bearings is reduced by the displacement of the rotor. However, for the calculation of the inertia, we have to use the total mass of the rotor. Theoretically, there is also a certain amount of water that is accelerated with the rotor by friction. Because the speeds are low, this additional mass is neglected in the present study.

AI.3.5 Weight estimate of rotor plus biomass

The dry weight calculation of the rotor is the sum of the weights of all the individual parts. These have been either calculated or weighed. The calculation of the mass of the biofilm is based on a maximum expected volume and an estimated density. Based on discussions with other researchers at Eawag, it is assumed that the biofilm will be between 2 and 3 mm thick and is evenly distributed over the discs. It is also assumed that the specific gravity of the wet biofilm is 900 kg/m3. Attached to this note is a calculation sheet with the figures for this reactor.

AI.3.6 Calculation of mass moment of inertia

The mass moment of inertia is calculated in reference to the central shaft of the rotor. For a solid cylinder, the mass moment of inertia around this axis is:

$$I = 1/2 \cdot m \cdot r^2 \qquad \textit{(Formula 3.1)}$$

With: I = moment of inertia round central axis (kg·m)
m = Mass of rotor (kg)
r = Radius of rotor (m)

AI.3.7 Torque required to start rotor

The required torque depends on the mass moment of inertia and on the rate of acceleration. The former is calculated as in formula 3.1. For the latter, one needs to estimate the time required to accelerate. Because the gear reduction in our machine is very big and the rotor speed is low, a short acceleration time is estimated: 2 seconds.

To calculate the angular acceleration, we first need to calculate the final angular velocity:

$$\omega = RPM \cdot 2\pi / 60 \qquad \textit{(Formula 3.2)}$$

With: ω = Rotational speed (rad·s^{-1})
RPM = Rotations per minute (-)

With the estimate acceleration time follows:

$$\alpha = \omega / t \qquad \textit{(Formula 3.3)}$$

With: α = Average angular acceleration (rad·s^{-2})
ω = Rotational speed (rad·s^{-1})
t = Acceleration time (s)

Now the required torque to accelerate the rotor can be calculated:

$$T_I = I / \alpha \qquad \textit{(Formula 3.4)}$$

With: T_I = Torque required to accelerate rotor (N·m)
Other parameters as calculated above

Torque required to start the rotor

Rotor mass			
Dry mass of rotor			
item	**mass**	**# items**	**total mass**
-	*kg*	-	*kg*
Disc with foam	0.25	48	12
PPR pipe and fittings	6.08	1	6
Steel pipes inside PPR pipes	10.13	1	10
Spacer clips	2	1	2
Total dry mass			**30**

Mass of growth on rotator	**value**	**unit**	**total mass**
Number of discs	48	-	
Disc diameter	650	mm	
Exposed area per disc	0.66	m^2	
Estimated thickness of growth	3	mm	
Total volume of growth per disc	1.99	dm^3	
Estimated density of wet growth	900	$kg \cdot m^{-3}$	
Mass of wet growth on one disc			1.79
Total mass of wet growth on rotor			**86**

Component mass	**value**	**unit**	**total mass**
PPR pipe and fittings length	16	m	
Mass per length	0.38	$kg \cdot m^{-1}$	
Total mass of PPR pipe and fittings			**6.08**
Steel reinforcements length	7300	mm	
Diameter	25	mm	
Thickness	2.5	mm	
Density	7850	$kg \cdot m^{-3}$	
Total mass of steel reinforcements			**10.13**

AI.4 Calculation note: *Drive unit, gearing and battery requirements*

AI.4.1 Introduction

This calculation note reports on the calculations made to design the drive system for the RBC and the required battery capacity.

Because we did not have the technical specifications of the wiper motor, we did a series of experiments to determine the maximum torque it can produce, its revolving speed and power consumption. Based on those, we estimated the torque and power for nominal working conditions.

With these data, we designed the gearing system and determined the required battery capacity.

AI.4.2 Conclusions

Based on the referenced calculations of the required torque and on the theoretical torque available, it can be concluded that the drive system will be powerful enough to turn the reactor, given that the belt drive does not slip. During testing, the current drawn by the motor was measured and found to be fluctuating. This because the resistance to buoyancy is not constant. The measured current uptake varied between 1.8 and 2.6 A, which means the battery capacity calculations are based on realistic values. The battery capacity is easily big enough to bridge the times of load shedding, though it is theoretically possible that the recharge time is too long, if the periods without power become longer than the periods with power supply.

AI.4.3 References

[1] STUN drawing 01-100-01: Arrangement anammox reactor

[2] STUN drawing 01-500-01: Reactor drive train arrangement

[3] STUN Calculation note: Total torque and power required

AI.4.4 Calculation input and assumptions

We measured the stall torque of the motor, which is the maximum torque that the motor can supply when you stop it turning. It is assumed that the maximum nominal working torque is 60% of this stall torque. We measured the power (Watt) that the motor draws when spinning freely. It is assumed that the power required under load is 1.5 times this power.

Since the drive consists of a belt and pulley system, some slippage of the belt will occur. As the speeds are low, this slippage should not be large. As the driver pulley is much smaller than the follower pulley, slippage will be more on the former pulley; slippage is assumed to be 5% and 2% respectively.

AI.4.5 Determining the motor properties

The motor output shaft has two preset speeds: 38 and 50 RPM. Free running, it draws 1.67 amperes at 12 Volts. The free running power is thus:

$$P = V \cdot A \quad (12 \cdot 1.67 = 20\ W) \qquad \textit{(Formula 4.1)}$$

With: P = Motor power consumption (Watt)
A = Ampere drawn by motor (A)
V = Motor voltage (V)

The motor stall torque was determined by attaching a lever to the output shaft and measuring the force (kg) required to stop the motor. This experiment was carried out 4 times and then the result was averaged. For the measurement data, see the attached calculation sheet.

The formula for determining the stall torque:

$$T_S = F_{av} \cdot g \cdot l \qquad \textit{(Formula 4.2)}$$

With: T_S = Stall torque of motor (N·m)
F_{av} = Average measured force (kg)
g = Acceleration of gravity ($m \cdot s^{-2}$)
l = Length of lever at which force is measured from centre of shaft (m)

Electric motors cannot operate at the stall torque. Based on generally accepted figures for electric motors, the maximum nominal workload is assumed to be 60% of the stall torque.

$$T_N = 0.6 \cdot T_S \qquad \textit{(Formula 4.3)}$$

With: T_N = Nominal work torque of motor (N·m)
T_S = Stall torque of motor (N·m)

AI.4.6 Gear ratio calculations

For reasons of availability of materials, ease of manufacturing and economics, the gearing between the motor and reactor rotor is done by means of a belt drive. The motor drives a small pulley, which is connected with a belt to a large pulley, which in turn is connected to the rotor. The full calculations are given in the attached worksheet. In this text, we will present the relevant formulas.

The first calculation is about the reduction in RPM by the belt drive:

$$RPM_2 = RPM_1 \cdot C_1 / C_2 \cdot (1 - \eta_1 - \eta_2) \qquad \textit{(Formula 4.4)}$$

With: RPM_1 = Revolutions per min. of driving shaft (-)
RPM_2 = Revolutions per min. of following shaft (-)
C_1 = Circumference of driving pulley (mm)
C_2 = Circumference of following pulley (mm)
η_1 = Efficiency of driving pulley (-)
η_2 = Efficiency of following pulley (-)

Since the circumference of both pulleys relates to the diameter of the pulleys according:

$C = D \cdot \pi$ *(Formula 4.5)*

With: C = circumference of pulley (mm)
D = Diameter of pulley (mm)

The formula for RPM reduction can also be stated as:

$RPM_2 = RPM_1 \cdot D_1 / D_2 \cdot (1 - \eta_1 - \eta_2)$ *(Formula 4.6)*

With: D_1 = Diameter of driving pulley (mm)
D_2 = Diameter of following pulley (mm)
Other parameters as above

Note: The diameters used should be the centreline of the belt on the pulley, rather then the inside of the groove of the pulley.

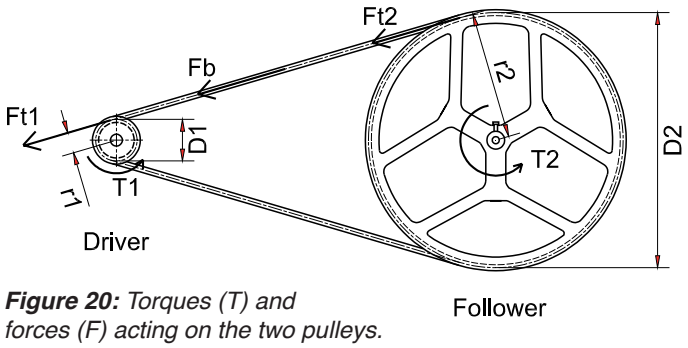

Figure 20: *Torques (T) and forces (F) acting on the two pulleys.*

While the rotating speed is reduced by the gear system, at the same time, the output torque is increased at the same rate. In Figure 20, the principle of this calculation is illustrated; the driver pulley is turned by torque T_1, as a result there is a tangential force (F_{t1}) at the rim of the pulley. If there is no slippage, F_{t1} is transmitted by the belt, as a pulling force in the belt (F_b), to the second pulley as F_{t2}. This force in turn creates a torque (T_2) on the shaft of the follower pulley. The relation between the torque and the tangential force is:

$T = r \cdot F_t$ *(Formula 4.7)*

With: T = Torque (Nm)
r = Radius of pulley (m)
F_t = Tangential force on pulley (N)

The pulling force in the belt is calculated as follows:

$F_b = F_{t1} = T_1 / r_1 \cdot (1 - \eta_1)$ *(Formula 4.8)*

With: F_b = Pulling force in the belt (N)
F_{t1} = Tangential force of edge of driver pulley (N)
T_1 = Input torque on driver pulley (Nm)
r_1 = Radius of driver pulley (m)
η_1 = Efficiency of driving pulley (-)

For the calculation of the torque on the follower shaft:

$T_2 = F_{t2} \cdot r_2$ *(Formula 4.9)*

With: T_2 = Output torque of follower shaft (Nm)
F_{t2} = Tangential force edge of follower pulley (N)
r_2 = Radius of follower pulley (m)

And:

$F_{t2} = F_b \cdot r_2$ *(Formula 4.10)*

Follows:

$T_2 = F_b \cdot \eta_2 \cdot r_2$ *(Formula 4.11)*

With: F_b = Pulling force in the belt (N)
η_2 = Efficiency of following pulley (-)
Other parameters as above

AI.4.7 Required battery capacity

In Kathmandu, there are two scheduled power cuts every day. As electricity is generated by hydropower, the length of the so-called load-shedding depends on the season. Based on last year's experience, two blocks of 8 hours without power are to be expected in the winter.

As is indicated in the referenced calculation notes, the predictions of the resistance and power required to run the reactor are not very accurate. To get some basis for the battery sizing, we have assumed that when working under load, the motor will draw 1.5 times the power as when running freely. The required power is dependent on both voltage and current according to:

$P = V \cdot A$ *(Formula 4.12)*

With: P = Power used by motor (Watt)
V = Voltage of motor (V)
A = Current drawn by motor (A)

Since the voltage for the system is a constant 12 volts, we can base the calculations on the current. The battery capacity is normally stated in ampere-hours (Ah). This is a measure of how many hours a battery could supply a current of 1 ampere. It should be noted that for reasons of battery life, it is recommended that only 30% of the theoretically available capacity is used.

To determine the required capacity:

$A_l = A_f \cdot 1.5$ *(Formula 4.13)*

With: A_l = Current drawn under load (A)
A_f = Current drawn free running (A)

$Ah_r = A_l \cdot t$ *(Formula 4.14)*

With: Ah_r = Required capacity to bridge blackout (Ah)
A_l = Current drawn under load (A)
t = Duration of blackout (load shedding) (h)

Drive unit, gearing and battery requirements

Motor power measurements	value	unit
Voltage	12	V
Current uptake (free running)	1.67	A
Estimated current uptake under load	2.51	A
Power uptake (free running)	20.04	W

Torque check	value	unit
Lever for torque measurement	200	mm
Measured pull experiment 1	2.5	
Measured pull experiment 2	2.0	
Measured pull experiment 3	2.0	
Measured pull experiment 4	3.0	
Average stall pull at 200mm lever	2.38	kg
Average stall pull at 200mm lever	23.3	N
Stall torque	4.66	Nm
Estimated nominal working torque	**2.80**	**Nm**

Motor torque	value	unit
RPM @ 12 volts	38	RPM
Motor power	20	W
Stall torque	4.66	Nm
Estimated nominal working torque	2.8	Nm
Estimated ampere under load	2.51	A

Belt drive properties	value	unit
Diameter drive wheel	35	mm
Circ. Drive wheel	110	mm
Estimated belt slip on driver pulley	5	%
Diameter follower pulley	430	mm
Circ. Follower pulley	1351	mm
Estimated belt slip on follower pulley	2	%
Output rotating speed	2.88	RPM

Torque calculation for follower shaft	value	unit
Tangential force on edge of driver pulley	152	N
Pulling force in belt	152	N
Tangential force on edge of follower pulley	152	N
Efficiency of belt on follower pulley	0.98	-
Torque on follower shaft	32.0	Nm

Motor properties	value	unit
Voltage	12	V
Current uptake (free running)	1.67	A
Estimated current uptake under load	2.51	A

Battery properties	value	unit
Battery capacity	80	Ah
Depth of discharge	30	%
Maximum usable capacity	24	Ah
Maximum duration of blackout	8	h
Required capacity	**6.28**	**Ah**

AI.5 Calculation note: *Resistance due to buoyancy*

AI.5.1 Introduction

As the rotor turns, parts of the rotor become submerged and move trough the effluent until they surface again. While submerged, the buoyancy force either helps to turn the rotor forward or works against the motion of the rotor. In the second case, the torque created by the buoyancy is part of the resistance that the rotor has to overcome. This note presents the calculations for this resistance and explains why the two halves of the rotor are offset by 90° from each other rather then being parallel.

AI.5.2 Conclusions

As the rotor turns, the buoyancy forces alternately accelerate and decelerate the rotor. The peak resistance due to buoyancy is calculated in this sheet (approximately 2.1 Nm). This value makes this component significant in relation to the other resistance components, but is much lower than the maximum value for a rotor with two parallel halves (approximately 6.7 Nm).

AI.5.3 References

[1] The calculations are based on widely accepted engineering mechanics formulas. These formulas can be found in the general domain.

[2] The input figures are based on STUN drawing 01-100-01 “Arrangement Anammox reactor” and referenced drawings.

AI.5.4 Buoyancy and resulting torque

The rotor is made out of a 3-dimensional pipe structure. When the rotor spins, the pipe elements move in and out of the liquid. As the pipes are closed, they displace an amount of liquid equal to their volume. In accordance with Archimedes law, the submerged pipe elements are subjected to a force – acting vertically upwards – that is equal to the mass of the displaced liquid.

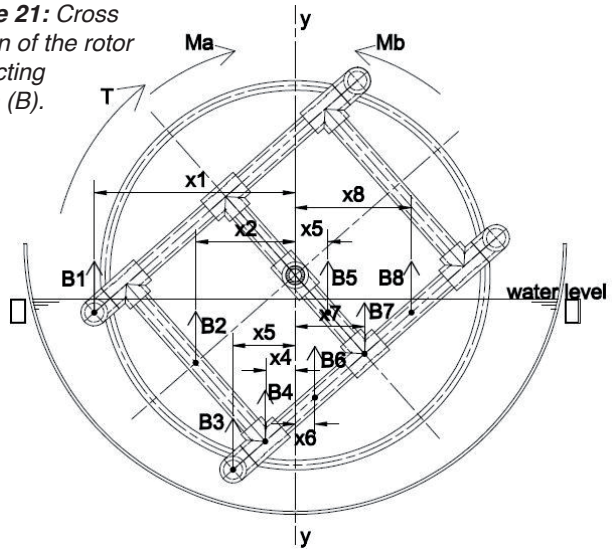

Figure 21: *Cross section of the rotor and acting forces (B).*

Because the pipe elements are not distributed evenly along the circumference of the rotor, the upward force due to buoyancy varies in amount and location during a turn of the rotor. In Figure 21, a cross section of the rotor is presented. The buoyancy forces of the various submerged parts of the rotor are indicated with the arrows (B_1 to B_8). Each force also has a dimension line with an x-coordinate from the line y-y. Each of the forces tries to turn the rotor along its central shaft (the z-z axis, perpendicular to the paper). This means each force has a moment around the central shaft. This moment is defined as the force multiplied by the distance to the turning point, measured perpendicularly to the direction of the force. For the moment caused by B_1:

$$M_1 = B_1 \cdot x_1 \qquad \textit{(Formula 5.1)}$$

With: M_1 = *Moment caused by force* B_1 *(Nm)*
B_1 = *Buoyancy force acting on part of rotor (N)*
x_1 = *Distance from central axis to force* B_1 *(m)*

For every other buoyancy force, a moment can be calculated in the same way. The central shaft is located on the y-y axis, so all the forces acting of the left side of y-y tend to turn the rotor clockwise, whereas the forces on the right hand side of y-y tend to turn it counter-clockwise. In the above figure, two moments are indicated: M_a and M_b these are the summations of the individual moments that try to turn the rotor clockwise and counter-clockwise respectively. These two moments partly cancel each other out, so the remaining moment is the torque (T) that is acting on the rotor shaft. All the individual moments are added up as presented in the table below to calculate the total torque. Note that the x-coordinates on the left of y-y are entered as negative values.

Force	Distance	Moment
N	*m*	*Nm*
B_1	$-x_1$	$M_1 = B_1 \cdot -x_1$
B_2	$-x_2$	$M_2 = B_2 \cdot -x_2$
B_3	$-x_3$	$M_3 = B_3 \cdot -x_3$
B_4	$-x_4$	$M_4 = B_4 \cdot -x_4$
B_5	x_5	$M_5 = B_5 \cdot x_5$
B_6	x_6	$M_6 = B_6 \cdot x_6$
B_7	x_7	$M_7 = B_7 \cdot x_7$
B_8	x_8	$M_8 = B_8 \cdot x_8$
	Torque =	**$M_1 + M_2 + M_3 \ldots M_8$**

The calculated value of the torque can be either positive or negative, i.e. it acts counter-clockwise or clockwise. If we assume that the rotor moves counter-clockwise, a negative torque value acts as a resisting force, whereas a positive torque value pushes the rotor forward. In addition to minimizing the resisting force, the force accelerating the rotor should also be minimized, in order to achieve a more constant resistance and a more regular rotation.

In the same way as the torque due to buoyancy, also a torque due to the weight of the rotor components can be calculated. However, if we look at both sides of the y-y axis, we see that for every part of the rotor, there is a part on the other side of the y-y axis with the same x coordinate and the same weight. As a result, the torque due to weight is always zero.

AI.5.5 Design modifications because of buoyancy

The forces B_1 and B_3 represent the buoyancy of the pipes in the longitudinal direction of the rotor. These are much larger than the buoyancy of the pipes that are visible in the cross section. In the situation depicted in Figure 21, a strong torque tends to turn the rotor counter-clockwise. In the original design, both halves of the rotor were parallel, creating a strong resistance due to buoyancy and causing problems for the drive unit. An improvement was made by offsetting one half of the rotor by 90°, as shown in Figure 22. As a better balance between the submerged parts of the rotor was established, resistance due to buoyancy decreased.

Figure 22: *Cross section of the rotor with offset halves.*

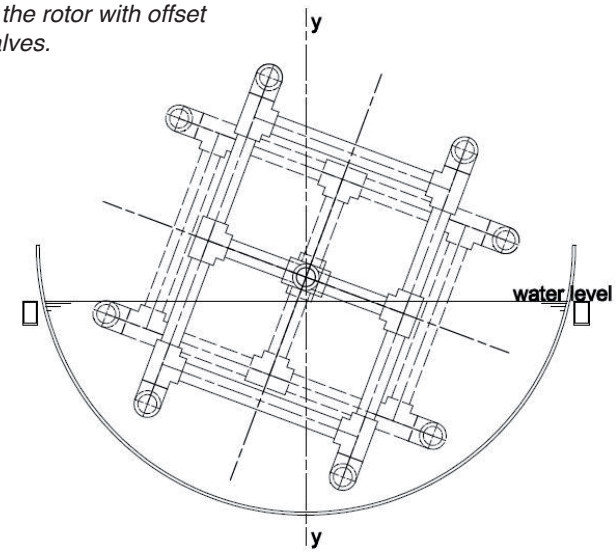

In the above figure, a cross section is given showing both rotor halves (one in a solid line and one in a dashed line). The situation presented in Figure 22 is also the situation in which the maximum resistance due to buoyancy occurs. This position of maximum buoyancy resistance was determined with a complicated calculation model, which approximates the buoyancy acting on the main longitudinal pipe elements in the rotor for every angle of rotation. As this calculation model is only an approximation, it was necessary to optimize the position of maximum torque graphically (turning the rotor in the drawing to the position in which it has the most torque as a result of the buoyancy). Given that the calculation model is only an approximation, but quite complicated and technical, it is not presented here. To illustrate the difference that the position of the rotor halves in respect to each other makes, two graphs from the above mentioned calculation model are presented in Figure 23: The plot compares the torque due to buoyancy as a function of the rotor's turning angle for the original

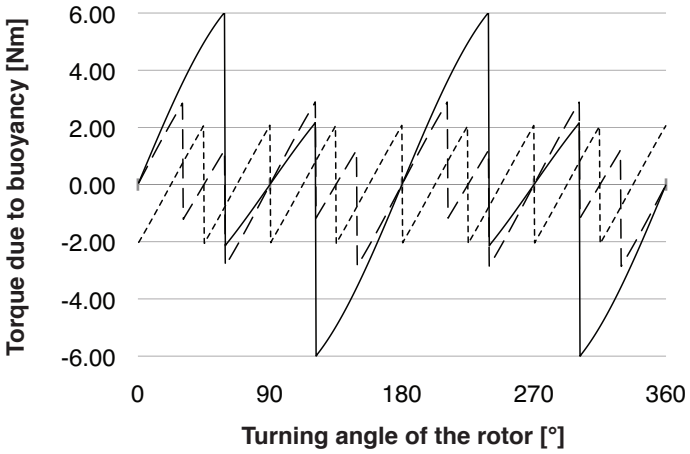

Figure 23: *Torque due to buoyancy – a comparison between rotor layouts:*

——— *rectangular rotor with parallel halves*

— — — *rectangular rotor with halves offset by 90°*

-------- *square rotor with halves offset by 45°*

design (both halves parallel) and for the new design with the offset rotor halves. A further reduction in torque could be achieved by changing the rotor design from a rectangular cross section of the rotor to a square. For an effective reduction in torque due to buoyancy, the halves of the rotor would have to be offset by 45° (90° does not affect squares).

AI.5.6 Calculation of resistance due to buoyancy

The calculation of the maximum resistance due to buoyancy for the RBC is calculated in the attached spreadsheet. Below an explanation and the formulas used. The difference in buoyancy force is also calculated in the spreadsheet. The figure on the calculation sheet represents the submerged part of the rotor. The buoyancy force acting on all parts are calculated for each part according to following formulas:

Volume of part under consideration:

$$V = l \cdot (\pi / 4) \cdot D^2 \cdot 10^{-6} \qquad \textit{(Formula 5.2)}$$

With: V = Volume displaced by part (L)
l = Length of part (mm)
D = Outside diameter of part (mm)
the factor 10^{-6} is to convert from mm^3 to litres

Buoyancy force acting on part:

$$F_B = V \cdot \rho \cdot g \qquad \textit{(Formula 5.3)}$$

With: F_B = Buoyancy force acting on part (N)
V = Volume displaced by part (L)
ρ = Density of water = 1 ($kg \cdot L^{-1}$)
g = Acceleration of gravity = 9.81 ($m \cdot s^{-2}$)

Resistance due to buoyancy

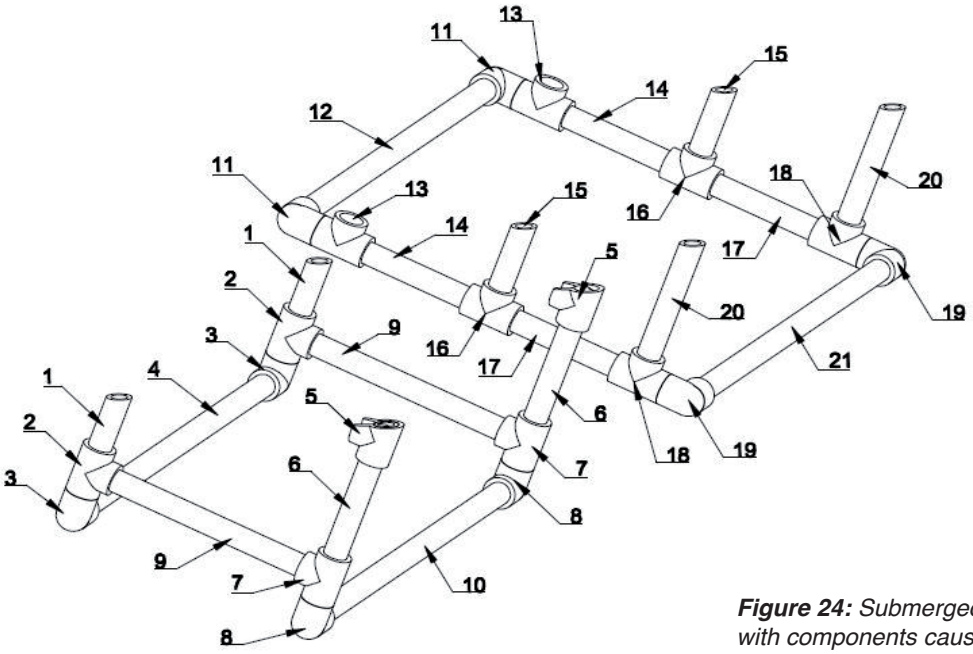

Figure 24: *Submerged part of the rotor with components causing buoyancy.*

#	Part	number of items	average length	outside diameter	volume	buoyancy	distance to shaft	moment
-	-	-	*mm*	*mm*	*l*	*N*	*mm*	*Nm*
Left half of rotor								
1	Left vertical pipe	2	77	32	0.12	1.13	-215	-0.24
2	Left bottom tee	2	85	40	0.21	1.94	-240	-0.47
3	Left bottom elbow	2	70	40	0.18	1.6	-266	-0.43
4	Left longitudinal pipe	1	690	32	0.55	5.05	-266	-1.34
5	Right middle tee	2	57	40	0.14	1.3	165	0.22
6	Right vertical pipe	2	150	32	0.24	2.2	125	0.27
7	Right bottom tee	2	85	40	0.21	1.94	87	0.17
8	Right bottom elbow	2	70	40	0.18	1.6	62	0.10
9	Bottom transverse pipe	2	280	32	0.45	4.1	77	0.32
10	Right longitudinal pipe	1	690	32	0.55	5.05	62	0.31
Right half of rotor								
11	Left bottom elbow	2	70	40	0.18	1.6	-335	-0.54
12	Left longitudinal pipe	1	690	32	0.55	5.05	-335	-1.69
13	Left bottom tee	2	85	40	0.21	1.94	-268	-0.52
14	Left bottom transverse pipe	2	150	32	0.24	2.2	-165	-0.36
15	Middle vertical pipe	2	105	32	0.17	1.54	-30	-0.05
16	Middle bottom tee	2	85	40	0.21	1.94	-61	-0.12
17	Right bottom transverse pipe	2	150	32	0.24	2.2	50	0.11
18	Right bottom tee	2	85	40	0.21	1.94	145	0.28
19	Right bottom elbow	2	70	40	0.18	1.6	213	0.34
20	Right vertical pipe	2	180	32	0.29	2.63	190	0.50
21	Right longitudinal pipe	1	690	32	0.55	5.05	213	1.08
Total								**-2.06**

AI.6 Calculation note: *Total torque and power required*

AI.6.1 Introduction

This calculation note documents how the various resistance components are added up, and how from this total resistance, the required power input is calculated. The formulas are given in the text, while the actual calculation and values are presented in the attached calculation sheets.

AI.6.2 Conclusions

The total (peak) torque required for the rotor is approximately 7.0 Nm, including friction of the bearings. At 3 RPM this means an energy input of approximately 2.3 W.

AI.6.3 References

[1] Stun Calculation note C01-002 “Rotor viscous resistance”

[2] Stun Calculation note C01-003 “Torque required to start rotor”

[3] Stun Calculation note C01-005 “Resistance due to buoyancy”

AI.6.4 Total required torque including bearing friction

In each of the referenced calculations [1], [2] , and [3], a part of the total resistance of the rotor is determined. This resistance is presented as a torque, which is required to overcome this part of the resistance. Therefore, the sum of all torques is the total resistance that the drive system has to overcome.

The approach of adding up all the components of the resistance is conservative, as the inertia component only occurs during start-up, while the buoyancy component varies during a rotation, and even has a negative value from time to time. The required torque and power calculated here is a maximum required. During operation, the resistance varies and is smaller than the calculated value .

The total required torque in the last stage of acceleration can be approximated as:

$$T = T_i + T_v + T_B + \eta_b \qquad \textit{(Formula 6.1)}$$

With: T = *Total torque during acceleration (Nm)*
T_i = *Torque to accelerate rotor (Nm)*
T_v = *Torque to overcome viscous resistance (Nm)*
T_B = *Torque to overcome buoyancy resistance(Nm)*
η_b = *Combined efficiency of bearings (-)*

For the combined efficiency of the bearings:

$$\eta_b = \eta^n \qquad \textit{(Formula 6.2)}$$

With: η = *efficiency of one bearing = 0.98 (-)*
n = *number of bearings on shaft (-)*

AI.6.5 Required power to overcome resistance

Above, the torque required to turn the rotor is calculated. With this, the energy required to turn the rotor a specified angle (in our case 1 full rotation) can be calculated. Because the time required for a rotation is also known, the power required for the reactor can also be determined.

Work done for one rotation:

$$E = \theta \cdot T \qquad \textit{(Formula 6.3)}$$

With: E =*Work done (J)*
θ = *Angular displacement = 2π (rad) for 1 rotation*
T = *Torque required (Nm)*

Required power:

$$P = E / t \qquad \textit{(Formula 6.4)}$$

With: P = *Required power (W)*
E = *Work done for one rotation (J)*
t = *Time required for one rotation (s)*

Time required for one rotation:

$$t = 60 / RPM \qquad \textit{(Formula 6.5)}$$

With: RPM = *rotations per minute of rotor (-)*

Parameter	value	unit
Reactor revolving speed	3	RPM
Time for one rotation	20	s
Torque required to overcome viscosity	3.88	Nm
Torque required to overcome buoyancy	2.06	Nm
Torque required to start rotor	1.03	Nm
Total required torque	6.97	Nm
Efficiency of individual bearings	0.98	-
Number of bearings on shaft	3	-
Combined efficiency of bearings	0.94	-
Torque required incl. bearing friction	7.41	Nm
Work done for one rotation	46.53	J
Energy required for one rotation	**2.33**	**W**

Appendix II Drawings

Drawings

All drawings are available as PDF or AutoCAD files (.dwg) on the STUN website:

www.eawag.ch/stun

Refer to the format specifications on the drawings (A2/A3/A4) for correct scale.

Low-cost Rotating Biological Contactor

Construction Manual

www.eawag.ch/stun

January 2011- Māgh 2067